Improvement in crystallinity of annealed V_2O_5 thin films deposited by spin coating technique for optoelectronic device applications

S. NITHYA, R. SENGODAN*
Department of Physics, Kumaraguru College of Technology, Coimbatore-49, India

Vanadium Pentoxide (V_2O_5) thin films were coated on a well cleaned glass substrate by spin coating technique. The coated films were characterized by XRD, EDS, SEM and UV – Vis. EDS is used to determine the elemental composition of a sample. By detecting the characteristic X-rays emitted by elements when they are excited by an electron beam, we can identify the elements present in V_2O_5 thin films and quantify their relative concentrations. SEM provides high-resolution images of the surface morphology of V_2O_5 thin films. This helps us to understand the surface features, such as roughness, grain size, and overall texture. XRD patterns revealed that the as a deposited film is in amorphous nature and annealed films is the polycrystalline nature with orthorhombic phase. UV-Vis spectra is used to explore the optical properties of the material, including transmittance, absorption coefficient, and extinction coefficient. From the absorption spectrum, the band gap energy of the material is calculated. The band gap of films is found to be 1.44 eV to 1.21 eV as deposited and annealed at 150 °C and 350 °C. The band gap values are decreased with increasing annealing temperature.

(Received November 16, 2023; accepted June 3, 2024)

Keywords: Spin coating, XRD, Grain size, Band gap energy

1. Introduction

V_2O_5 is a transition metal oxide with the most stable oxidation state of V^{5+}. This stability is due to its saturated oxidation state, making it an interesting material for various applications. V_2O_5 exists in different polymorphs, including α, β, γ, and δ phases. Among these, the orthorhombic α-V_2O_5 is the most stable phase [1]. V_2O_5 has found applications in a wide range of fields, such as chemical sensing, optoelectronics, batteries (as a cathode material), electrochromic devices, and catalysis [2]. This is due to its unique properties, including a multi-layer structure, wide optical bandgap, good chemical and thermal stability, and excellent electrical and thermal properties. In the context of solar cells, V_2O_5 is used as an electrode material. In optoelectronics, thin films of V_2O_5 are employed in the fabrication of light-emitting diodes (LEDs) and other devices. V_2O_5 thin films possess high electrical conductivity, high optical reflectivity, and a low dielectric constant, making them suitable for energy-saving applications such as smart windows and clothing [3]. V_2O_5 undergoes a reversible change from being an insulator to a conductor when exposed to light or heat which makes it useful for applications were switching between these two states is desired. For example, V_2O_5-based window coatings can reflect heat when the outside temperature is high, preventing the building from using air conditioning. In the winter season when the outside temperature is low, it may allow sunlight to enter, thus heating the interior naturally. This same property can also be utilized in smart clothing. Such characteristics and rationale compelled us to concentrate on a deeper investigation of the surface and microstructure characteristics of V_2O_5 as most of the above-mentioned applications depend on these two characteristics. Moreover, it is necessary to monitor crucial optical factors that are connected to diverse technological applications. Due to the desirable properties and applications, over the last few decades, synthesis of V_2O_5 thin film has attracted great attention. Such as chemical vapour deposition [4, 5], pulsed laser deposition [6, 7], thermal evaporation [8], ultrasonic spray deposition [9], magnetron sputtering [10, 11], spray pyrolysis [12] and spin coated [13]. Each method has its own advantages and is suited for different purposes. Due to its advantages, including high purity, homogeneity, stoichiometry, simplicity of equipment, and cost-effectiveness for coating large surface areas, the spin-coating process has emerged as one of the most effective methods for depositing metal oxide thin films. Recently, there has been a notable surge in research focused on investigating the structural and optical properties of V_2O_5 thin films using the spin-coating technique. In this current study, we delve into the structural, morphological, and optical characteristics of spin coated V_2O_5 thin films at different annealing temperatures.

2. Experimental technique

2.1. Materials

Vanadium pentoxide (V_2O_5) films are prepared on a glass substrate by the spin coating technique. 1g of vanadium pentoxide powder was dissolved in 25 mL of distilled water. The resulting solution is stirred for 5 hours at constant temperature by using magnetic stirrer.

2.2. Preparation of V_2O_5 thin films

The vanadium pentoxide films were deposited using spin coating technique on glass substrate. Prior to the coating process, the glass substrates were cleaned by using soap solution and then with distilled water to remove any impurities present. The cleaned substrate is heated at 100 °C for an hour. The films were coated on the treated substrate with an rpm of 1800 for 80 seconds. The samples were annealed in air at 150 °C and 350 °C for an hour.

2.3. Characterization

2.3.1 X-ray diffraction (XRD) analysis

The structure of the hybrid thin films was analysed by using X-ray diffraction (XRD) analysis using Bruker AXS D8 advance diffractometer having CuKa (λ= 1.5406 A) radiation with value of 2θ ranged from 10^0 to 80^0 operating voltage of 40 kV and a current of 30 mA.

2.3.2 Scanning electron microscopy (SEM-EDS) analysis

The surface morphology was studied by using JEOL Model JSM-6390LV scanning electron microscopy (SEM). The elemental composition of films was determined using the JEOL Model JED-2300 energy dispersive X-ray analysis (EDS).

2.3.3 UV-visible-NIR spectrophotometry

The optical properties were studied for the wavelength range of 350 nm to 2500 nm with a resolution of 0.1 nm by using a UV-Vis-NIR (JASCO V-670, Japan) spectrophotometer.

3. Result and discussion

3.1. EDS analysis

Fig. 1 show the EDS spectra of V_2O_5 films annealed at different temperatures. It appears that the EDX spectra of V_2O_5 films annealed at different temperatures have confirmed the presence of elements that are expected in the structure of V_2O_5 thin films. Specifically, elements like V (Vanadium) and O (Oxygen) have compositions that are closer to the stoichiometric ratio in V_2O_5 thin films. Additionally, the EDS spectrum indicates the absence of any impurities, which is a positive result.

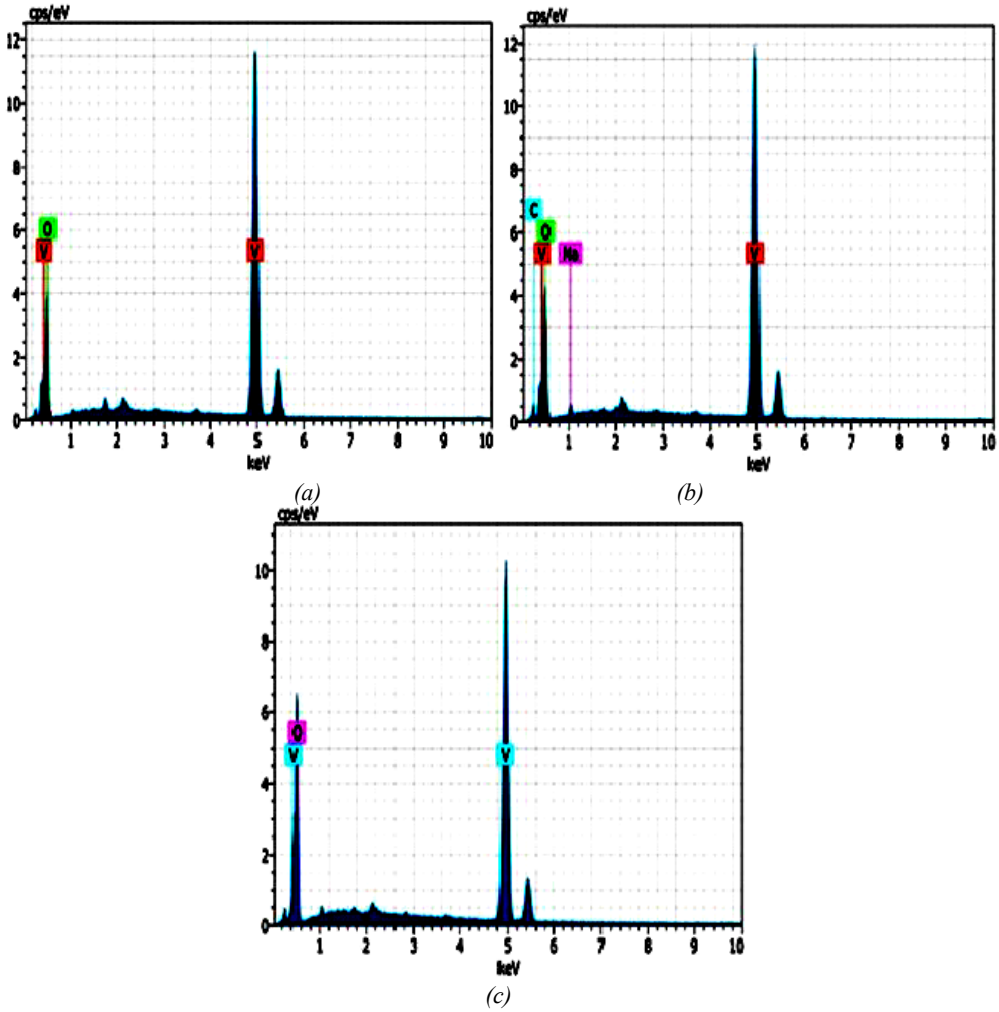

Fig .1. EDS spectra of V_2O_5 films (a)As de, (b) annealed at 150° C (c) annealed at 350° C

Table 1 presents the comparative composition percentages of V and O in the thin films at different annealing temperatures. Notably, it is observed that the concentration of oxygen atoms increases as the temperature of annealing is raised.

Table 1. EDS spectra of V_2O_5 films annealed at different temperatures

Temperature	Elements	Mass %	Atomic %
As deposited	V	68.97	41.11
	O	31.03	58.89
150°C	V	66.75	38.67
	O	33.25	61.33
350°C	V	60.43	32.42
	O	39.57	67.58

3.2. Morphology study

Fig. 2 shows the FESEM images of the V_2O_5 thin films as deposited and different annealing temperatures. As-prepared films exhibit the formation of rod-like structures on the film surface. This indicates a specific microstructure that forms during the initial preparation phase. At an annealing temperature of 150°C, there is a transition in the morphology. Randomly oriented rod structures are observed on the surface, suggesting that the annealing process influences the microstructure. The film annealed at 350°C shows the formation of platelet structures with various dimensions [14]. This further highlights the influence of annealing temperature on the resulting microstructure. Notably, there are no pits, pinholes, or dendritic features found on the surface. This suggests a relatively smooth and defect-free surface. Increasing temperature promotes surface diffusion, enabling atoms or molecules to migrate across grain boundaries. This process reduces the number of boundaries and encourages the growth of larger grains. Consequently, as temperature rises, grain size increases due to enhanced mobility and rearrangement of particles, a fundamental aspect in materials science.

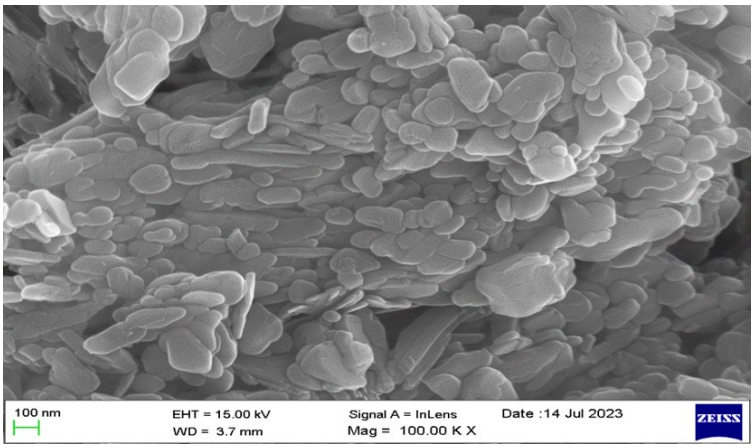

As Deposited

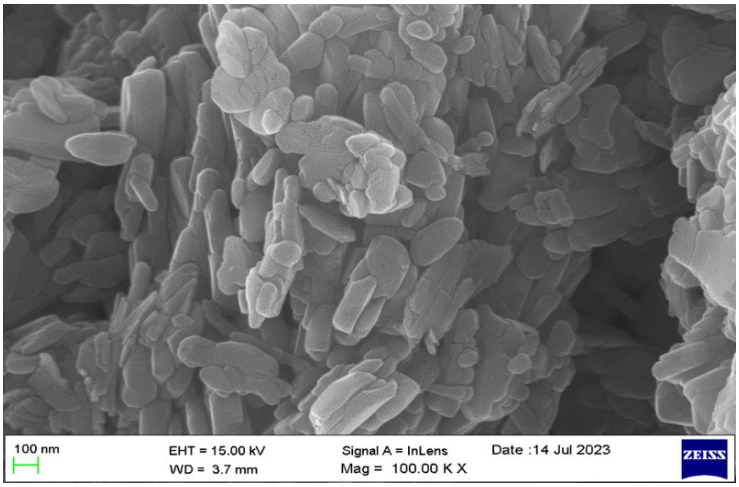

Annealed at 150°C

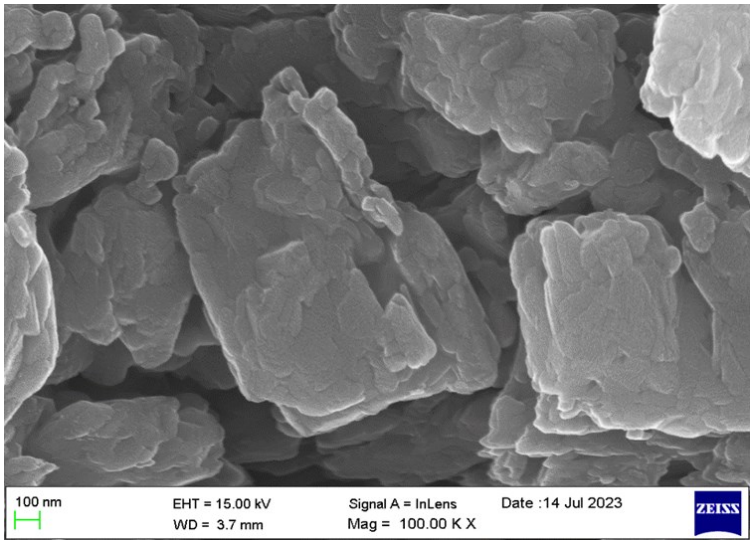

Fig. 2. FESEM images of the V_2O_5 thin films as deposited at different annealing temperatures

3.3. X-ray diffraction analysis

The X-ray diffractograms of as deposited and annealed thin films of V_2O_5 are shown in Fig. 3. As-deposited films exhibit an amorphous nature, indicating a lack of long-range order in the atomic arrangement. All annealed films show a transition to a polycrystalline structure with an orthorhombic crystallographic arrangement [15], and all the reflections are indexed using ICDD card 04-007-1156. This suggests a transformation from an amorphous to a crystalline state due to the annealing process. The X-ray diffractograms reveal that the intensity of the (400) peak increases as the annealing temperature rises. This indicates a higher degree of orientation along the (400) crystallographic plane. The position of the (400) peak becomes more intense with increasing annealing temperature, confirming a high level of crystalline growth in the V_2O_5 films. The structural parameters like crystalline size, lattice parameters, dislocation density, and micro strain were calculated using the below formulae, and the results are presented in Table 2.

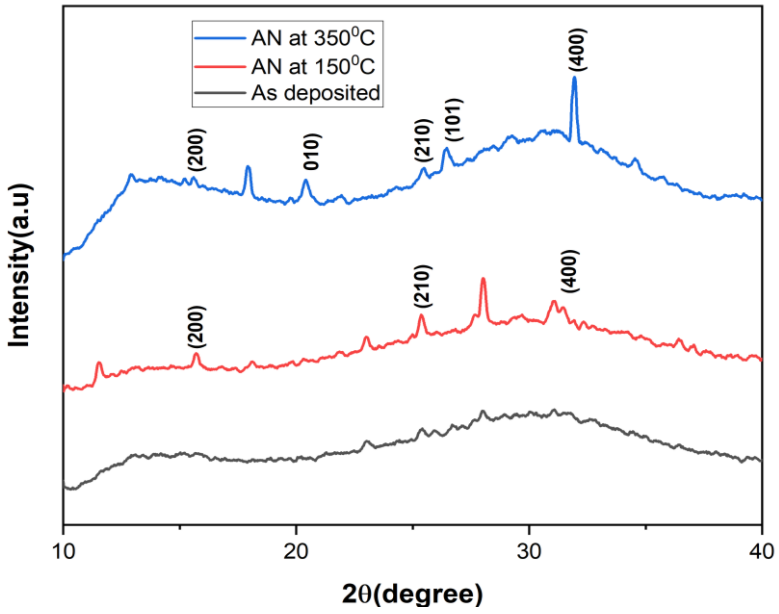

Fig. 3. X-ray diffractograms V_2O_5 thin films annealed at different temperatures (color online)

The average crystallite size (D) was calculated using the Scherrer's formula [16]

$$D=\frac{K\lambda}{\beta\cos\theta} \quad (1)$$

β – Full width half maximum of the corresponding XRD peak at radiant.
K – constant (≈0.94).
Θ – Bragg's angle
λ – wavelength of X-ray

The dislocation density (δ), which represents the number of defects in the crystal, is estimated from the equation,

$$\delta = \frac{1}{D^2} \quad (2)$$

Strain (ε) of the thin film is determined from the following formula,

$$\varepsilon = \frac{\beta \cos\theta}{4} \quad (3)$$

Table 2 indicates that the crystalline size of the films increases with higher annealing temperatures. This is attributed to the agglomeration of small grains, resulting in larger grains. The micro strain and dislocation density are indicators of defects in thin films. These values decrease with increasing annealing temperature, suggesting an improvement in the crystalline quality and a reduction in defects [17]. Overall, the annealing process has led to the production of high-quality thin films with good crystalline characteristics and low dislocation densities. The effective grain size increases, and the defect density decreases. Notably, films annealed at 350°C have produced the best crystalline and high-quality thin films.

Table 2. Structural parameters of V_2O_5 thin films

Annealing temperature (˚C)	2θ (Degrees)	hkl	Crystalline size (nm)	Strain (ε) x10^{-4} ($lin^{-2}m^{-4}$)	Dislocation density (δ) 10^{14}(lin/m^2)
150	15.426	200	53.10	6.53	3.54
	25.625	210	48.49	7.14	4.25
	31.567	400	56.94	6.08	3.08
350	15.426	200	59.48	5.83	2.83
	25.625	210	97.05	3.57	1.06
	31.567	400	92.77	3.74	1.16

3.4. Optical properties

The transmittance spectrum of the V_2O_5 thin films as deposited and annealed at different temperatures were measured over the wavelength range 350-2500 nm is shown in Fig. 4. It is observed that as deposited film showed maximum transmittance of 58% whereas annealed films showed maximum transmittance of 61% and 63% for 150°C and 350˚C. It can be clearly seen that the transmittance increases with increase of annealing temperature [18]. The increase in the transmission with annealing temperature may be due to the decrease in number of defects, increase of crystallite size improvement in surface morphology of the respective films. The observed increase of optical transparency upon annealing temperature could be attributed to the formation of high crystallinity and smooth surface with less defect states resulted in decrease of optical scattering. Low transmittance observed in the lower wavelength range, and it increases toward increase in the higher wavelength range [19]. The observed decrease in transmittance in the lower wavelength range may be due to band gap absorption of material.

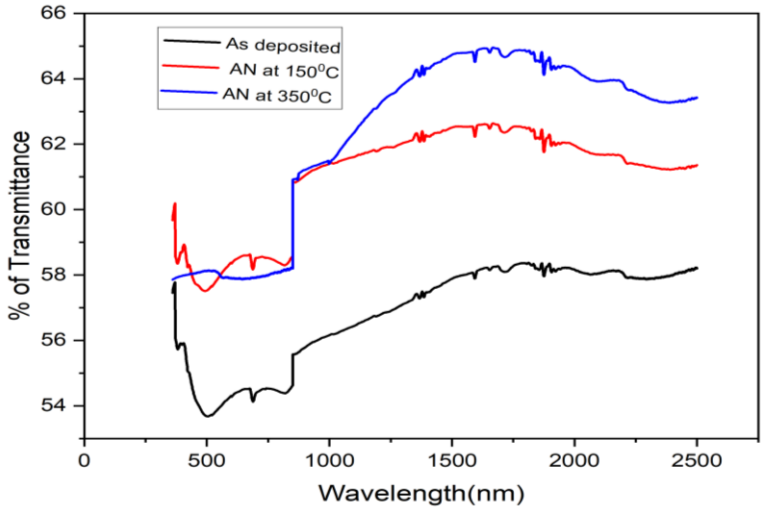

Fig. 4. Transmittance spectrum of the V_2O_5 thin films annealed at different temperatures (color online)

From the transmittance data, the extinction coefficient (k) was calculated using the following relation.

$$k = \frac{2.303 log_{10}\left(\frac{1}{T}\right)\lambda}{4\pi t} \quad (4)$$

where t is the thickness of film and T is the transmittance.

The absorption coefficient (α) was calculated using the following relation.

$$\alpha = \frac{4\pi k}{\lambda} \quad (5)$$

where λ is the wavelength of the incident radiation and k is the extinction coefficient. In addition, the optical absorption coefficient, α is related to the energy band gap and is given by the equation.

$$\alpha \propto [h\upsilon - E_g]^m \quad (6)$$

where $h\upsilon$ and E_g are the photon energy and the optical energy gap respectively. In this expression, the values of m are $\frac{1}{2}$ and 2 for direct and indirect transition respectively.

The refractive index is a crucial optical parameter for materials. It is wavelength-dependent and describes how electromagnetic radiation interacts with the material. When electromagnetic waves pass through a material medium, they can incur losses. These losses include scattering of photons, phonons (vibrational quanta in a crystal lattice), and free carrier absorption. The refractive index is of paramount importance in the design of integrated optical devices. This includes devices like switches and filters. The refractive index determines how light propagates through and interacts with the device. The refractive index is also a critical parameter in electrochromic devices. These are devices that change colour or opacity in response to an applied voltage. The Swanepoel method is highlighted as an adaptive and accurate technique for determining the refractive index of thin films and the corresponding relation is described as follows [14,20]

$$n = [H + (H^2 + S^2)^{1/2}]^{1/2} \quad (7)$$

where H is the Swanepoel coefficient

$$H = \frac{4S^2}{(S^2+1)T^2} - \frac{S^2+1}{2} \quad (8)$$

where s is the refractive index of the substrate (1.5 for glass) and T is the interference free transmittance

The variation of extinction coefficient (k) as a function of wavelength for different temperatures is shown in Fig. 5. From the plot it is seen that the k value increases with increase of wavelength, which is due to interbrand transition between the valance and conduction bands. It is also seen that the k values are decreasing with increase of annealing temperature. This is possibly due to various factors. Primarily, higher annealing temperatures facilitate better crystallinity and grain growth, reducing defects and impurities that contribute to absorption and scattering of light, thereby decreasing the extinction coefficient. Additionally, improved film morphology and smoother surfaces at higher temperatures can also lead to reduced light absorption and scattering, further lowering the extinction coefficient. The extinction coefficient values varying from 0.53 to 0.45. The obtained low value of k implies that fraction of light loss due to scattering for both as deposited and annealed films which indicates that the prepared thin films have very low absorption [17].

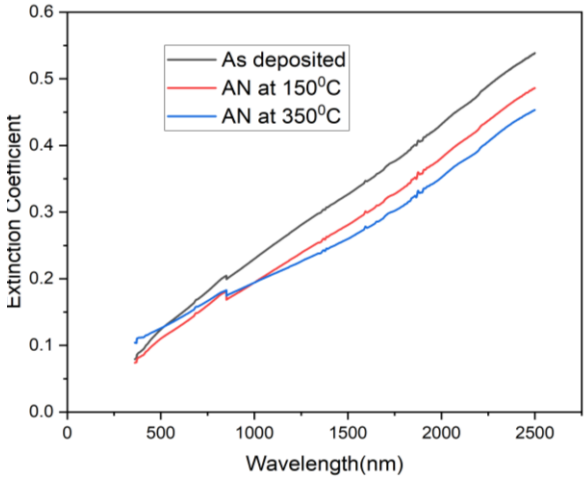

Fig. 5. Extinction coefficient of the V_2O_5 thin films annealed at different temperatures (color online)

Fig. 6 shows the absorption coefficient (a) versus wavelength at different temperature. The observation that the absorption coefficient decreases with an increase in annealing temperature suggests that as the material is subjected to higher temperatures (annealing), its optical properties change. This change could be due to defects in the material being modified during annealing. The absorption coefficient is related to the band gap of a material. The band gap is the energy difference between the valence band and the conduction band in a solid-state material. It determines the material's electrical and optical properties. In particular, the band gap affects how a material absorbs and emits light. When the absorption coefficient (a) is greater than 10^{-4} cm ^{1}, it suggests the occurrence of a direct optical transition. In a direct transition, an electron in the valence band absorbs a photon of energy and is excited directly into the conduction band, without intermediate states. This can be a useful criterion for determining the nature of the optical transitions in a material.

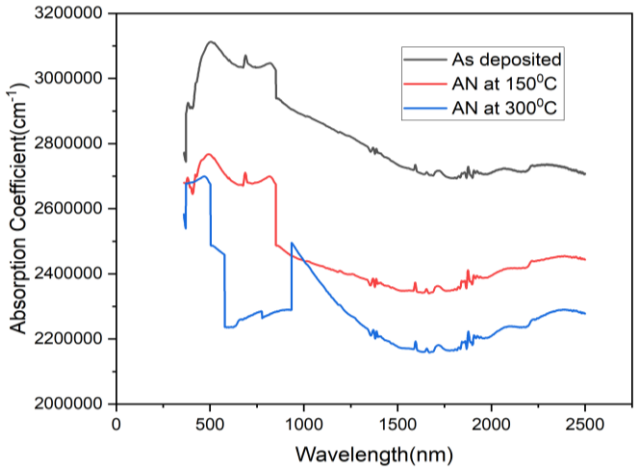

Fig. 6. Absorption coefficient of the V2O5 thin films annealed at different temperatures (color online)

The band gap energy (Eg) was estimated using Tauc's plot by extrapolating the linear portion of the $(\alpha h\nu)^2$ versus hν curve to the x-axis, which is shown in Fig. 7. The bandgap value was estimated with n = 2, which is related to the direct bandgap region. Extrapolating the linear region of Tauc plot to zero absorption coefficient gives the band gap of the films. The estimated band gap energy values are 1.44 eV, 1.38 eV and 1.21 eV for as deposited and annealed at 150°C and 350°C. The band gap values are decreased with increasing annealing temperature [1]. It may be due to the quantum confinement effect, increasing of the crystallinity and decreasing of the dislocation densities of V_2O_5 thin films [21-24].

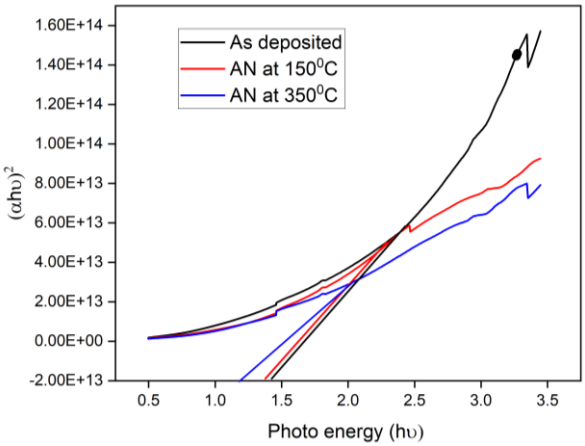

Fig. 7. $(\alpha h\nu)^2$ with hν of V_2O_5 thin films annealed at different temperatures (color online)

Fig. 8. shows the refractive index (n) versus wavelength of as deposited and annealed films. The obtained refractive index values decrease with increase in annealing temperature [25]. Different annealing temperatures can result in different levels of crystallinity or defects in the film, which in turn influence its decrease in refractive index. In the visible region of the electromagnetic spectrum, the refractive index typically increases with increasing wavelength. This behaviour is associated with the material's interaction with light in the visible spectrum. The increase in refractive index as wavelength increases can be related to the dispersion of light, where different wavelengths of light travel at different speeds in the material, leading to a change in the refractive index. In the NIR region, the refractive index generally decreases with increasing wavelength. This behaviour can also be explained by the material's electronic structure. NIR light has lower energy compared to visible light, and its interaction with the material's valence and conduction bands may result in a decrease in refractive index with increasing wavelength. This phenomenon is often associated with the electronic band structure of the material.

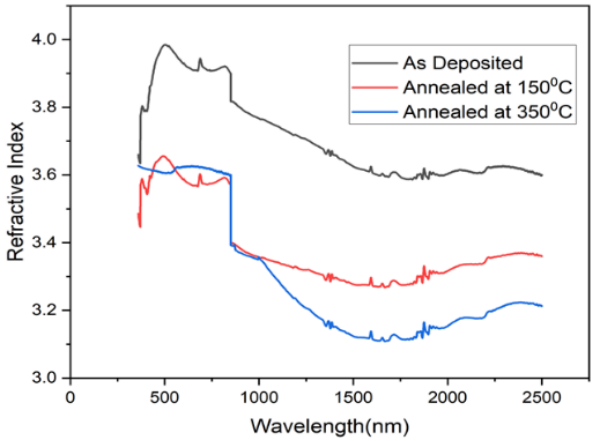

Fig. 8. Refractive index of V_2O_5 thin films annealed at different temperatures (color online)

4. Conclusion

V_2O_5 thin films were deposited using the spin coating technique. The annealing temperature had a significant impact on both the structural and optical properties of the V_2O_5 thin films. The presence of vanadium and oxygen was confirmed by Energy Dispersive X-ray Spectroscopy (EDS). The XRD patterns indicated that the as-grown film was amorphous. After annealing, the films exhibited a polycrystalline structure with an orthorhombic phase. The intensity of the diffraction peaks increased as the annealing temperature increased, suggesting improved crystallinity. Field Emission Scanning Electron Microscopy (FE-SEM) images revealed a rod-like shaped surface in the V_2O_5 films. The optical spectra showed that transmittance values increased with higher annealing temperatures, indicating improved crystallinity. The films exhibited excellent transmittance and low absorbance. The optical parameters such as band gap and refractive index of the films decrease with increasing annealing temperatures. The results suggest that the deposited V_2O_5 thin films, with their excellent transmittance, low absorbance, smooth surface, and polycrystalline structure, hold promise for use in transparent optoelectronic device applications in the near future.

References

[1] Bhanu Priya, Priya Jasrotia, Indra Sulania, Dhirendra K. Chaudhary, Rajeev Gupta, Ajay Singh Verma, Raj Kumar, Tanuj Kumar, ECS Advances **2,** 02100 (2023).

[2] B. Li, Y. Xu, G. Rong, M. Jing, Y. Xie, Nanotechnology **17**, 2560 (2006).

[3] Sergey Burdyukh, O. B. A. Pergament, Adv. Condens. Matter Phys. **2**(2), 9789370 (2018).

[4] Dimitra Vernardou, Coatings **7**(2), 24 (2017).

[5] N. K. Nandakumar, E. G. Seebauer, Thin Solid Films **519**, 3663 (2011).

[6] C. V. Ramana, R. J. Smith, O. M. Hussain, C. C. Chusuei, C. M. Julien, Chem. Mater. **17**, 1213 (2005).

[7] P. K. Jain, M. Salim, D. Kaur, Optik **126**, 3260 (2015).

[8] R. Santos, J. Loureiro, A. Nogueira, E. Elangovan, J. V. Pinto, J. P. Veiga, T. Busani, E. Fortunato, R. Martins, I. Ferreira, Appl. Surf. Sci. **282**, 590 (2013).

[9] Y. Wei, M. Li, J. Zheng, C. Xu, Thin Solid Films **534**, 446 (2013).

[10] I. Quinzeni, S. Ferrari, E. Quartarone, P. Mustarelli, J. Power Sources **196**, 10228 (2011).

[11] L. J. Meng, R. A. Silva, H. N. Cui, V. Teixeira, M. P. dos Santos, Z. Xu, Thin Solid Films **515**, 195 (2006).

[12] R. Irani, S. M. Rozati, S. Beke, Mater. Chem. Phys. **139**, 489 (2013).

[13] V. Balasubramani, J. Chandrasekaran, R. Marnadu, P. Vivek, S. Maruthamuthu, S. Rajesh, Journal of Inorganic and Organometallic Polymers and Materials **29**, 1533 (2019).

[14] Arul Carolin Amala, Ravi Vignesh, Gobalakrishnan Vasanthi Geetha, Rengasamy Sivakumar, Phys. Status Solidi A **2100282**, 1 (2021).

[15] Semih Incecam, Adem Sarac, Evren Erdil, Ali Orkun, Cagirtekin, Selim Acar, J. Sci, Part A **8**(2), 299 (2021).

[16] R. Sengodan, B. Chandar Shekar Bellan, J. Optoelectron. Adv. M. **22**(5-6), 280 (2020).

[17] Ravinder Gandasiri, C. J. Sreelathaa, P. Nagarajub, Y. Vijayakumar, Physica B: Condensed Matter **572**, 220 (2019).

[18] Anchal Rana, Aditya Yadav, Govind Gupta, Abhimanyu Rana, RSC Adv. **13**, 15334 (2023).

[19] Sathish Sugumaran, Chandar Shekar Bellan, Dinesh Muthu, Sengodan Raja, Dinesh Bheeman, Ranjithkumar Rajamani, RSC Adv. **5**, 10599 (2015).

[20] N. Ushaa R. Sivakumar, C. Sanjeeviraja Y. Kuroki, J. Appl. Phys. **649**, 112 (2015).

[21] Bakr F. Hassan, Mohammed J. Dathan, Anas A. Abdallah, Iraqi Journal of Science. **62**(10), 3536 (2021).

[22] Ravinder Gandasiri, C. J. Sreelatha, P. Nagaraju, Y. Vijayakumar, Physica B: Condensed Matter **572**, 220 (2019).

[23] S. Sathish, B. Chandar Shekar, S. Chandru Kannan, R. Sengodan, K. P. B. Dinesh, R. Ranjithkumar, International Journal of Polymer Analysis and Characterization **20**, 29 (2015).

[24] D. Vasanth Raj, N. Ponpandian, D. Mangalaraj, C. Viswanathan, Materials Science in Semiconductor Processing **16**, 256 (2013).

[25] S. W. Xue, X. T. Zu, W. L. Zhou, H. X. Deng, X. Xiang, L. Zhang, H. Deng, Journal of Alloys and Compounds **448**, 21 (2008).

*Corresponding author: sengodan.r.sci@kct.ac.in